

RECENT ADVANCES IN AIRFRAME-PROPULSION CONCEPTS WITH DISTRIBUTED PROPULSION

**A.T. Isikveren¹, A. Seitz¹, J. Bijewitz¹, M. Hornung¹, A. Mirzoyan², A. Isyanov²,
J.-L. Godard³, S. Stückl⁴, J. van Toor⁴**

¹Bauhaus-Luftfahrt e.V., 80807 München Germany

²Central Institute of Aviation Motors, 111116, Moscow, Russia

³ONERA, The French Aerospace Lab, F-92190 Meudon, France

⁴Airbus Group, 81663 München Germany

Keywords: *distributed propulsion, numerical aerodynamics, optimization, aircraft design*

Abstract

This paper discusses design and integration associated with distributed propulsion as a means of providing motive power for future aircraft concepts. The technical work reflects activities performed within a European Commission funded Framework 7 project entitled Distributed Propulsion and Ultra-high By-Pass Rotor Study at Aircraft Level, or, DisPURSAL. In this instance, the approach of distributed propulsion includes one unique solution that integrates the fuselage with a single propulsor (dubbed Propulsive-Fuselage Concept, PFC) as well as a Distributed Multiple-Fans Concept (DMFC) driven by a limited number of engine cores – both targeting entry-in-service year 2035+. The strong coupling between airframe aerodynamics and motive power performance is analysed using high-end, low-fidelity and interlaced-fidelity methods. Although this paper reflects work-in-progress results, initial indications show for a PFC undertaking medium-to-long-range operations around 9% reduction in CO₂-emissions compared to an evolutionary, year 2035, conventional morphology gas-turbine aircraft appears to be a worthwhile target.

1 Introduction

One of the ambitious goals outlined in Flightpath 2050 by the European Commission (EC) for year 2050 is a 75% reduction in CO₂-emissions per passenger kilometer (PAX.km)

relative to the capabilities of aircraft in the year 2000 [1]. 90% NO_x-emissions and 65% noise reductions are also advocated.

Targets for CO₂-emissions as defined in AGAPE 2020 [2] were categorised into Airframe, Propulsion and Power System (PPS), Air Traffic Management and Airline Operations. Subsequent to this the Strategic Research and Innovation Agenda (SRIA) goals [3] have been re-calibrated to reflect the AGAPE 2020 report and a new medium-term goal for Entry-into-Service (EIS) year 2035 has been declared, which is a significant point for aircraft fleet renewal. Further elaboration of these chronologically assigned CO₂-emissions targets are offered by way of breakdowns that recommend aircraft energy level targets.

Ref. [4] discussed growing evidence indicating for Airframe and PPS the projected cumulative impact of currently active and previous EC and National Framework Programmes will fall short by at least 8% of the year 2035 target (51% CO₂-emissions per passenger.km reduction) given in the SRIA document. If one extends the comparative exercise to include appreciation of SRIA 2050, there is a likelihood the outcome will be in greater deficit, namely, 15% away from the 68% CO₂-emissions reduction goal.

By considering an innovative propulsion systems integration approach and coupling this to the utilisation of alternative architectures, a possibility in closing this gap is surmised to occur. New degrees-of-freedom could arise where the propulsion system can be fully or

partially embedded within the airframe in an effort to exploit the benefits of Boundary Layer Ingestion (BLI) and/or Wake Filling, thus giving scope to reducing power requirements through improvements in propulsive efficiency. Such novel approaches necessitate a departure from the conventional, disparate, weakly-coupled airframe-propulsion combination and requires treatment of the design problem in a truly holistic sense with emphasis placed upon maximising synergy from the outset.

1.1 The DisPURSAL Project

The EC has recognised the potential benefits afforded by distributed propulsion solutions by granting approval for a Level-0 Framework 7 project entitled Distributed Propulsion and Ultra-high By-Pass Rotor Study at Aircraft Level, or, DisPURSAL [5]. Coordinated by Bauhaus Luftfahrt e.V., this 2-year project, which commenced in February 2013, involves partners from the CIAM (Russia), ONERA (France) and Airbus Group Innovations (Germany). The Consortium benefits from an Industrial Advisory Board comprising representatives from Airbus Group (Germany), MTU Aero Engines AG (Germany), DLR (Germany) and ONERA (France).

Targeting an EIS of 2035 this project investigates aircraft concepts employing distributed propulsion with focus placed upon one novel solution that integrates the fuselage with a single propulsor (dubbed the Propulsive-Fuselage Concept, or, PFC) as well as Distributed Multiple-Fans Concept (DMFC) driven by a limited number of engine cores. Aspects that are being addressed include aircraft design and optimisation, airframe-propulsion integration, power-train system design and advanced flow field simulation.

2 Multi-disciplinary Design of Distributed Propulsion Systems

A coherent, standardized and robust set-up in conjunction with adherence to strict procedural controls is needed to ensure successful multi-disciplinary interfacing, sizing and optimisation. Some details about numerical methods

employed for the aero-airframe-propulsion experimental work and a brief overview of multi-disciplinary interfacing are presented.

2.1 Down-selection Framework

During the down-selection exercise concept clouds comprising 6 candidate designs for both the PFC and DMFC sets were qualitatively rated against a total of 29 criteria which were grouped into 6 main categories with a technical, operational and certification related focus:

- Systems Integration;
- Aerodynamics;
- Weights;
- Noise;
- Operability and Certifiability; and,
- Costs

Each main category included a set of 4 to 7 specific sub-categories. The weightings of the main and sub-categories were tailored to reflect the emphasis placed upon fuel burn and cost reduction. Thus, those of the main categories having a major impact on fuel burn (“Systems Integration”, “Aerodynamics” and “Weights”) as well as the cost-influencing category (“Costs”) were each weighted with 0.20. The two remaining main categories (“Noise” and “Operability and Certifiability”) were each weighted with 0.10. The rating was attained by evaluation of each individual concept against what was intuitively deemed the best design candidate from within the pool of 6. In addition, technical maturity was assessed by evaluating each concept with respect to the likelihood of success and the effort to bring the technology to target TRL 6 by technology freeze in year 2030. Following the procedure described in Ref. [6], robustness of the concept rating was gauged by systematically varying the criteria weighting in each main category. This was achieved by means of artificial amplification in such a way one category was rated with 0.30 and the remaining weightings were equally distributed amongst the other categories.

2.2 Aero-Airframe Numerical Methods

The aerodynamic assessment of the airframe-propulsion was planned to be done for cruise

conditions and an important aspect was to represent correctly the phenomenon of BLI by the engine intake and the modification of the flow going through the engine fan. Due to this, the ONERA elsA software [8], being a high fidelity method solving the RANS equations, was selected. This software can treat a large variety of configurations and flow conditions. It can handle multi-block structured meshes and includes patched grid and overset capabilities, as well as state of the art numerical methods and advanced physical models. Several types of turbulence models can be used and, in the frame of the DisPURSAL project, the Spalart-Allmaras was used in fully turbulent conditions.

Due to the limited time and budget afforded by the project, the configurations considered were 2D-axisymmetric (see Fig. 2A) and 2D (see Fig. 2B) for PFC and DMFC respectively. An extrapolation of the aerodynamic performance coefficients was further performed to quantify the effects on a fully 3D configuration.

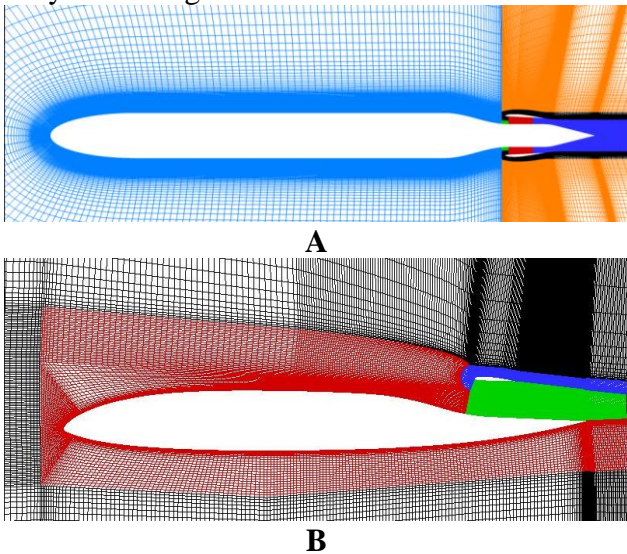


Fig. 2: (A) 2D-axisymmetric and (B) 2D configurations and aerodynamic meshes

It should be noted that only the engine fan was simulated, and not the engine core flow; the objective being mainly to evaluate the effect of BLI on the fan. It was not possible to calculate a real fan in the frame of the project, so the influence of the fan on the flow, including the modification of its characteristics when crossing it, has been simulated through specific numerical boundary conditions.

Two types of actuator disk conditions were used for 2D-axisymmetric and 2D configurations: the first one applies an increase of pressure through the fan while conserving the flow velocity; the second one is more advanced and based upon a fan characteristics deck which has to be provided by the user. It applies a total pressure and temperature drop as well as an azimuthal deviation of the flow. This later condition was applied in two planes at different streamwise positions in order to simulate a Contra-Rotating Open Rotor (CROR) fan. In order to build fan characteristics information to represent realistic fans, preliminary computations were performed with a code based on Glauert theory for propellers and extended to ducted fans, thus giving for a simplified fan blade skeleton and a given rotation speed the variations of flow characteristics necessary for the actuator disk boundary conditions.

Aerodynamic performance analysis was based on mass-flow through the engine, the power delivered by the fan to the flow and the net thrust of the engine, from which a propulsive efficiency can be deduced. These different parameters were obtained through integral operators comprising variables of local mass-flow, enthalpy and dynalpy over a selected surface in the field, in accordance with an approach developed for the RAPRO project [9].

2.3 Aero-Propulsion Numerical Methods

One of the challenges associated with highly integrated propulsion systems as analyzed in the DisPURSAL Project is rooted in the ingestion of a low-momentum boundary layer into the propulsive device and the corresponding influence on engine performance.

The momentum deficit formed by fuselage skin friction in front of the power plant intake of a PFC arrangement manifests as a total pressure loss relative to the total pressure of the undisturbed free stream at flight velocity [10]. Hence, ram pressure recovery for the BLI power plants is typically reduced compared to the value of an engine installed in free stream. For the PFC investigations, the method for the mapping of stream tube losses presented in Ref. [10] was initially utilised. In succeeding studies,

the results of more sophisticated numerical methods (see Section 2.2 and Section 4.2) suitable for the identification of important flow properties at relevant stations of the airframe and the propulsive device are incorporated.

As a further consequence of tightly coupled propulsion-airframe arrangements, the fan polytropic efficiency is expected to be reduced due to the inevitable distortion of the inflow field of a boundary layer ingesting power plant [10]. In the first instance, constant degradation factors were applied to fan efficiency as described in Ref. [11].

2.4 Aerodynamics/Propulsion Book-keeping

Different from vortex-induced drag, viscous and form drag, particularly the low-momentum boundary layer flow caused by skin friction on wetted areas, are manifested as a momentum deficit in the aircraft wake. Through the application of momentum and energy conservation laws it may be easily shown that locally filling this momentum deficit using a momentum delta produced by the propulsion system yields a reduction in propulsive power required for aircraft operation [10]. The consistent treatment of conventionally installed, i.e. podded, and, highly integrated propulsion systems such as the PFC requires a unified standard for the definition of the efficiency chain through the entire power plant system, as well as appropriate interfacing to the airframe.

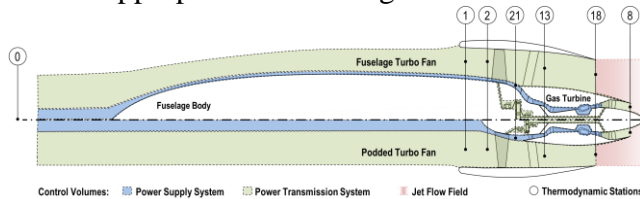


Fig. 3: Unified propulsion system definition based on standardised control volumes [10]

A unified book-keeping scheme of system-level efficiency figures and corresponding control volumes applicable to both conventionally podded, as well as, highly integrated BLI propulsion systems was introduced in Ref. [10]. Accordingly, the interface for thrust/drag book-keeping between the propulsion system and the airframe is geared to the propulsion system stream tube of air flow

(Fig. 3, above). Therefore, aerodynamic effects in the stream tube ahead of the inlet frontal face are incorporated in the power plant sizing and performance analysis. Nacelle external aerodynamics are considered to contribute to the overall aircraft characteristics, thereby, feeding back to the net thrust required to operate the aircraft, $F_{N,t}$. Knowing $F_{N,t}$, the net thrust requirement for each individual power plant may be derived. Assuming a certain amount of aircraft drag captured inside the propulsion stream tube (and ingested into the propulsive device), D_{ing} , the actual net thrust requirement of the aircraft, $F_{N,t}^*$, is reduced accordingly [10]:

$$F_{N,t}^* = F_{N,t} - D_{ing} \quad (1)$$

2.5 Multi-disciplinary Interfacing Procedures

General aircraft characteristics including principal dimensions, aerodynamic polars, weights, propulsion system characteristics, and flight performance are determined in a pre-conceptual design process based upon a set of initial assumptions and utilisation of mostly semi-empirical methods. On this initial basis, detailed shapes defining the aircraft Outer Mold Lines are created in a Computer-Aided Design (CAD) environment.

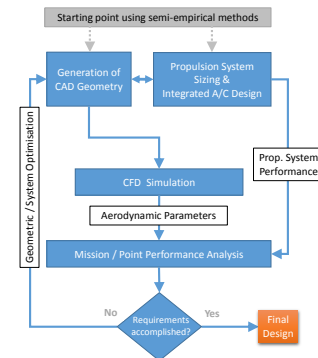


Fig. 4: Workflow scheme of the multi-disciplinary design process

In combination with preliminary results regarding propulsion system characteristics and performance, numerical flow simulations are conducted on these CAD shapes to investigate airframe-propulsion interaction effects and the overall propulsive efficiency. Potentially occurring flow imperfections like unfavorable shock contours or flow separations are addressed in this iterative geometrical

procedure. Results of the flow simulation are finally used to verify and subsequently calibrate the methods and assumptions used in the overall aircraft design and sizing models. An illustration of the applied workflow is given in Fig. 4 (previous page).

3 DisPURSAL Project Aircraft Top-Level Requirements and Reference Aircraft

Benchmarking of both distributed propulsion concept designs is performed against reference aircraft comprising major-systems and airframes reflecting in-service year 2000 and an evolutionary extrapolation of the contemporary state-of-the-art for target EIS of 2035. Together with account of future technical requirements and objectives a description of the reference aircraft is discussed below.

3.1 Aircraft Requirements and Objectives

Declaration of the application scenario and Aircraft Top Level Requirements (ATLeRs) forms the basis for the subsequent investigation of an advanced reference aircraft reflecting technology freeze-year 2030 and the distributed propulsion concepts. Based upon analysis of published data given in Ref. [12] it was found medium-to-long range stage lengths have the greatest impact on overall air transport system level cumulative fuel consumption. Using forecasts up to and including year 2035 [13], it was deduced 95% of the flights within this broad market segment can be performed with a cabin capacity of 320 to 340 seats. Accordingly, a design range of 4800 nm (8890 km) with payload of 340 passengers (PAX) in a 2-class arrangement was selected (see Fig. 5).

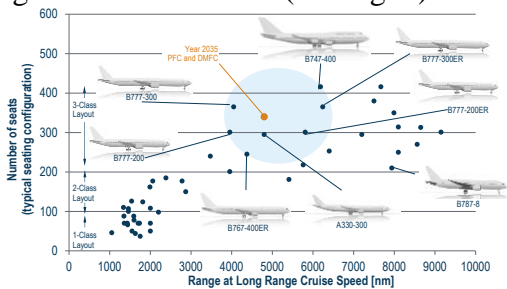


Fig. 5: Targeted market segment of entry-into-service 2035 advanced transport study

The complete array of ATLeRs entries tallied 18 line-items. For sake of brevity a summary of principal ATLeRs is given in Table 1.

Table 1: Principal Aircraft Top Level Requirements

Technology-Freeze / Entry-into-Service	2030 / 2035
Design Range and Accommodation	4800 nm 340 PAX
External Noise and Emission Targets (Datum year 2000, SRIA 2035)	CO ₂ -60% NO _x -84% Noise-55%
Take-off Field Length (MTOW, SL, ISA)	≤ 2300 m
Second Segment Climb	340 PAX, DEN, ISA+20°C
Landing Field Length (MLW, ISA)	≤ 2000 m
Approach Speed (MLW, SL, ISA)	≤ 140 KCAS
Airport Compatibility Limits (ICAO Annex 14)	Code E (52 m < x < 65 m)

Sizing of structures and systems of the PFC and DMFC is performed according to a product family strategy allowing for margin of future potential stretch and shrink derivatives of the baseline aircraft. Thus, the propulsion systems, for example, needs to be sized for the stretch version and the baseline and shrink version employing successive 10% thrust derates.

3.2 Year 2000 and 2035 Reference Aircraft

The selection of the reference aircraft was based upon the targeted application scenario and ATLeRs presented in Section 3.1. For purposes of gauging the relative merits of the PFC and DMFC to that of SRIA 2035 targets, an appropriate transport aircraft reflecting an in-service year 2000 standard needed to be defined and analysed. As this air transport task is, today, typically serviced by a wide-body medium-to-long-range twin-engine aircraft, an Airbus A330-300 equipped with Rolls-Royce Trent 700 power plants was chosen as the State-of-the-Art Reference (SoAR) aircraft. Hence, a parametric model of the aircraft including the corresponding propulsion system was fashioned.

In order to appropriately capture the benefits of the distributed propulsion concepts and to establish a suitable basis for consistent benchmarking, a reference aircraft reflecting the advanced technology level corresponding to an EIS 2035 application scenario was derived from the SoAR (designated as “2035R”). Design

range and payload were set in accordance with the ATLeRs given previously. Besides adjustments of the fuselage design relative to the SoAR in order to provide the required accommodation and future comfort standards, a set of aerodynamic, weights reduction and propulsion system related technologies appropriate for the targeted EIS was implemented.

An advanced flexible wing featuring an aspect ratio of 12.6, which was sized to match the ICAO Annex 14 Code E airport compatibility limit yielding a lift-to-drag (L/D) improvement of 8.6% (at $C_L = 0.50$, $M0.80$, FL350) over the SoAR was generated. With regards to the structural design, advanced technologies such as omni-directional ply orientation of carbon fibers and advanced bonding techniques were assumed to motivate a reduction of 15% in structural weight relative to the SoAR.

The aircraft is powered by advanced Geared Turbofan (GTF) power plants with a Bypass Ratio of 18.0. Cycle properties, turbo component efficiencies and duct pressure losses were adjusted to reflect the targeted technology standard.

In view of an aircraft systems architecture complying with the All-Electric Aircraft (AEA) paradigm, propulsion system design was based upon a zero customer off-take scenario with regards to cabin bleed air and electrical power extraction enabled by a Proton Exchange Membrane, fuel cell-based Auxiliary Power Unit. This resulted in a Thrust Specific Fuel Consumption (TSFC) improvement at typical cruise of 21.5% over the Trent 700 series installed on the SoAR.

In terms of mission performance, the 2035 reference aircraft was predicted to deliver a 32% block fuel benefit compared the SoAR carrying a payload of 340 PAX at 102 kg per PAX.

4 Propulsive Fuselage Pre-Concept Design

This section is devoted to presenting milestone achievements and the work-in-progress multi-disciplinary design results, findings and technical insights associated with the PFC design.

4.1 Initial Exploration and Down-selection

As part of the initial exploration phase, a comprehensive literature survey was conducted in order to gather state-of-the-art knowledge and technological solutions regarding the PFC. Variations of the PFC idea found in literature include the configuration proposed by Bolonkin [14] utilising an open rotor fan located just behind the wing root intended to maximize the propulsor area and to enable low specific thrust and thus high propulsive efficiency. Another idea is the “VoltAir” concept [15], a study in which an electrically powered ducted propeller installed at the aft fuselage provides BLI capability. Schwarze, moreover, proposed a configuration featuring a system of CRORs encircling the fuselage in front of the wing [16].

Based on the literature analysis, several conceptual morphologies considered indicative of a PFC concept were identified. The derived pool of architectural categories included:

- General Aircraft Architectures: PFC based on conventional tube and wing design, box-wing configuration and twin-fuselage design
- Propulsor Options: Single and multi-stage ducted fan, as well as unducted single and CROR configurations
- Drive-train Concepts: Mechanical power transmission, hydro-mechanical transmission using gas turbine exhaust gas and a power turbine to drive the Fuselage Fan (FF), as well as electro-mechanical power transmission
- Internal Gas-turbine Arrangement: Engines installed in front and aft of the FF plane
- Redundancy Implementation: FF in conjunction with under-wing podded power plants, double-bubble configuration and twin-fuselage layout each using two independently driven FFs

As a result of the down-selection process, the most promising candidate for the implementation of a PFC concept was identified: a concept featuring a single FF driven by a gas-turbine installed in the fuselage aft cone. It was also assessed to be a concept with the highest potential to meet the target technical maturity level compared to the other rated alternatives. In order to adequately address

system redundancy stipulated by transport category certification requirements, the configuration additionally comprises two under-wing podded ultra-high bypass ratio turbofans. An isometric view of the PFC aircraft is visualised in Fig. 6.

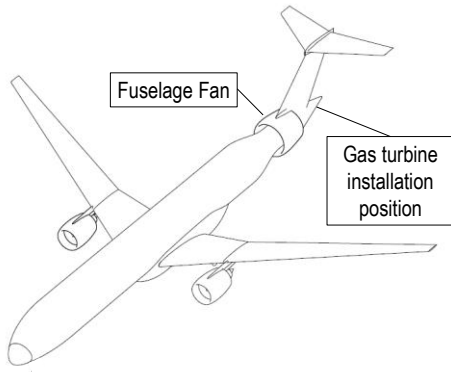


Fig. 6: Isometric view of down-selected Propulsive-Fuselage aircraft morphology

Selection of the empennage arrangement included the evaluation of stability and control aspects, flow interference issues in the aft fuselage section, as well as assessment of structural integrity. A major challenge for empennage integration emanates from the path of aft fuselage-induced mechanical loads being disrupted by the FF rotor [11]. As tail plane aerodynamic and inertial forces must be structurally transferred across the rotor plane, a number of unconventional empennage options were initially considered.

Apart from the conventional, T-tail, Butterfly and U-tail arrangements, the pool of evaluated options ranged from self-trimming C-wing solutions [17] to chin-mounted rudder and canard configurations as proposed in Ref. [18]. In order to avoid ramp safety issues and additional complexity of nose landing gear integration potentially associated with a fuselage underside nose-mounted empennage while ensuring minimum flow disturbance upstream of the FF, a T-tail solution was considered the most suitable option for the PFC aircraft. A T-tail reduces the complexity of structurally integrating the nacelle and tail planes. It avoids major interference between the fan inflow field and the control surfaces, and, provides sizing benefits of the vertical fin due to end plate effect as well as a larger lever arm for the horizontal stabiliser.

4.2 Aero-Airframe Numerical Experimentation

As a first step design activity, the rear fuselage and the nacelle were modified only in order to obtain a reference geometry reaching the desired thrust and engine mass-flow at cruise. This activity was followed by a sensitivity study with regards to aerodynamic and engine operating conditions. In a second step, the influence of geometric parameters such as the engine fan diameter was assessed.

Due to the fuselage length and rear engine installation, a thick boundary layer is ingested by the engine intake, as shown in Fig. 7 (local total pressure / freestream static pressure < 1.52). It clearly illustrates the increase of total pressure generated by the fan, as well as the low direct influence of the fan on the local Mach number (M), mainly driven by the engine mass-flow and the cross section streamwise evolution.

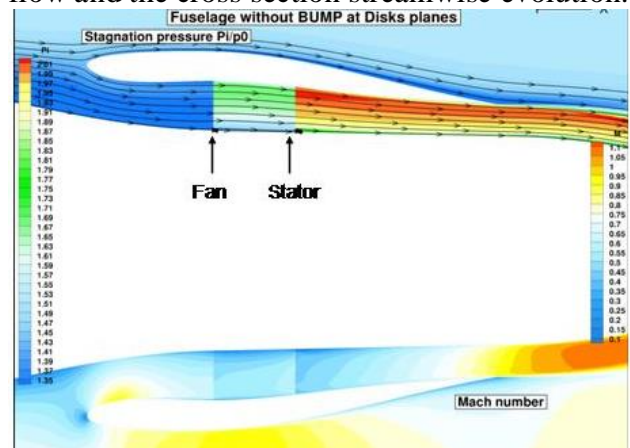


Fig. 7: Stagnation pressure (upper portion) and Mach number (lower portion) for the reference configuration at cruise condition

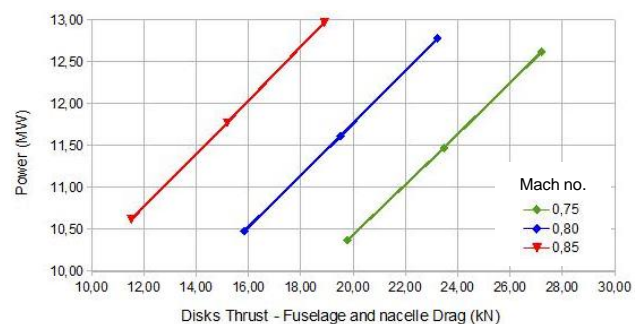


Fig. 8: Engine power versus net thrust for various power settings and Mach numbers

Engine power necessary to generate the target net thrust is shown in Fig. 8 above for

different power settings or flight M. At cruise (M0.80, FL350, ISA) , the reference shape has reached the objectives (power 12.0 MW, net thrust 21.0 kN). As expected, an increase of engine power is necessary to increase the thrust for a given M. Similarly, an increase in power is required to get the same net thrust if M is increased, due to drag increase. At cruise, the Fan Pressure Ratio (FPR) is equal to 1.47.

The influence of geometrical parameters, such as engine diameter has also been assessed, but only preliminary results are available at the moment. Fig. 9 clearly illustrates for a similar net thrust there exists risk of “blockage” in the nozzle with reduced diameter. A nozzle redesign is recommended for such conditions.

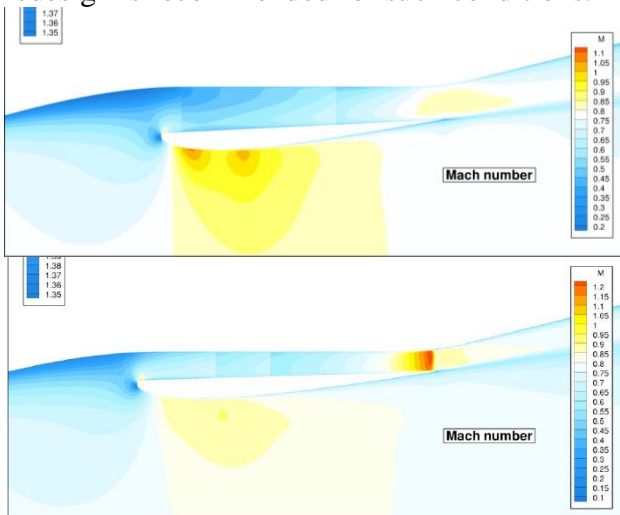


Fig. 9: Mach number evolutions for a reference (top) and a reduced (bottom) engine diameter at cruise

The latest numerical work is displayed in Fig. 10, showing friction lines at the surface of the fuselage (and friction modulus), pressures at the surface of the nacelle and flow streamlines.

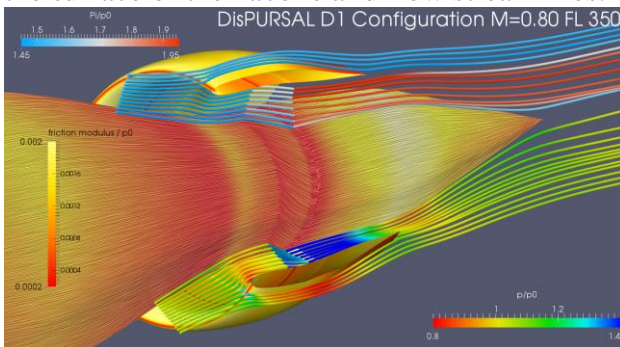


Fig. 10: Friction lines, pressures and flow streamlines of the Propulsive Fuselage

4.3 Power Supply and Transmission

According to the results obtained from the down-selection process, a single rotating FF device was chosen because of reduced complexity regarding mechanical and structural integration compared to other rated alternatives. A shrouded FF was preferred over an open rotor arrangement for noise reasons, and, superior robustness against tail strike [11] (see Fig. 11).

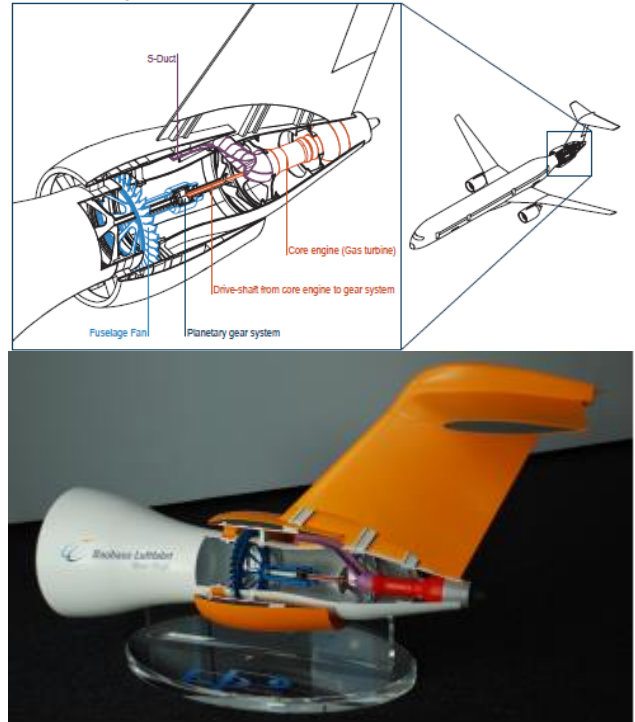


Fig. 11: Isometric CAD view and scaled physical mock-up of Fuselage Fan device

While in principle one could envision a hybrid-electric drive-train solution for a targeted EIS 2035, the main objective of the project phase described in the present paper was set on the evaluation of a mechanical power-train concept. Therefore, the FF is powered by the low-pressure spool via a planetary reduction gear system. The air supply of the turbo-engine is realized through an eccentric swan neck intake integrated in the FF bypass duct at the root of the vertical fin.

4.4 Initial General Arrangement, Specifications and Technologies Description

An initial three-view of the PFC aircraft is presented in Fig. 12 (overleaf).

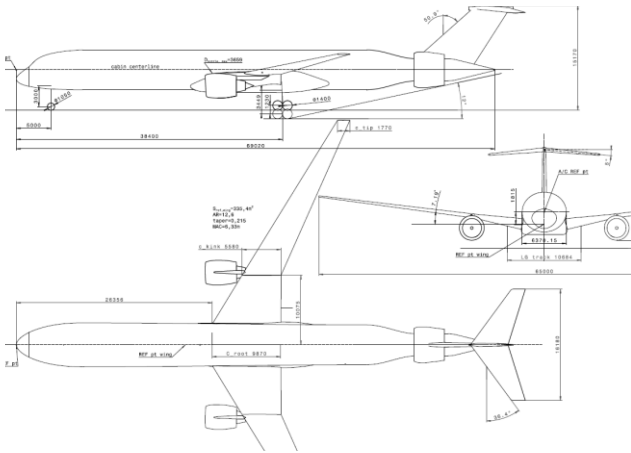


Fig. 12: Initial three-view of the Propulsive-Fuselage concept

A synopsis of important aircraft characteristics for the selected PFC design and the 2035R aircraft is given in Table 2.

Table 2: Comparative synopsis of important aircraft characteristics

		2035R	PFC	Δ [%]
Fuselage Length	m	67.0	69.0	+3.0
Wing Span	m	65.0	65.0	0.0
MTOW	kg	206230	206470	+0.1
OWE	kg	123462	127838	+3.5
Wing Ref. Area, S_{ref}	m ²	335.4	335.4	0.0
MTOW/ S_{ref}	kg/m ²	615	615	0.0
Thrust to Weight (SLS, MTOW)	-	0.31	0.30	-2.2
Fuselage Share of Total Cruise Drag*	%	25.4	25.3	-0.4
Ingested Drag Ratio = $D_{ing}/F_{N,t}$	%	n/a	21.0	n/a
Lift-to-Drag Ratio ($C_L=0.55, M=0.80$)	-	22.5	27.3	+21.3
Block Fuel Burn, 4800 nm, 340 PAX	kg	41690	37973	-8.9

*if BLI / wake-filling effects are not accounted

Based upon the down-selected general layout of the PFC morphology initial sizing and subsequent performance evaluation was conducted. While the FF encircling the aft fuselage behind the rear pressure bulkhead at 85% relative fuselage length is primarily intended to ingest the fuselage boundary layer, and thus serve the purpose of Wake Filling, residual thrust required to operate the aircraft is provided by the power plants installed under the wing. Axial positioning of the FF was driven by the intent of maximizing fuselage drag ingestion while providing appropriate fan disk burst corridors not interfering with critical tail

functions or the pressurised cabin. In order to accommodate identical cabin capacity as the 2035R, the fuselage length was increased by 2.0 m relative to the reference in order to account for the axisymmetrical contraction of the aft fuselage towards the FF inlet.

For the horizontal tail, a 5° anhedral was selected. The tail scrape angle was calculated with 12° with the main landing gear extended, thus also accounting for margin regarding a potential stretch version of the aircraft.

The design net thrust between both power plant types installed in the aircraft was iteratively determined in order to allow for commonality between the core engines. As a result, the thrust required for the podded power plants is reduced by approximately one third relative to the reference yielding a decrease in fan diameter. The final net thrust split for this iteration of sizing was approximately 73% for the under-wing podded and 27% for the FF.

Based on the calculation methods presented in Ref. [10], an ingested drag ratio, $D_{ing}/F_{N,t}$, of 21.0% resulted. Associated with this is a relative loss in propulsion system efficiency of 25% due to BLI (viscous wake flow with reduced momentum and strong non-uniformities in the flow). Despite the aforementioned detrimental effects on the performance of the FF propulsion system, a reduction in block fuel burn of 8.9% relative to 2035R and 37.1% relative to SoAR was obtained. This improvement compares favourably with results published in the past [7]. The removal of a significant share of fuselage drag out of the aircraft drag book-keeping yields a substantial increase in cruise lift-to-drag ratio.

As seen in Table 2, the structural weight of the PFC increases relative to the reference. This results from the increased fuselage length, the installation of the FF power plant at the aft-fuselage, the greater area of the horizontal tail to balance the aircraft pitching moment leading to an increased weight of the horizontal tail, and, fuselage and fin structural reinforcement required due to increased bending moments. In effect, the Operational Weight Empty (OWE) increases by 3.5%. Due to the significant fuel saving, however, Maximum Take-Off Weight (MTOW) remains almost constant.

5 Distributed Multiple-Fans Pre-Concept Design

The DMFC design is still very much a work-in-progress activity. This section provides a detailed overview of down-selection, it offers some insights gained from preliminary numerical aerodynamics work and presents initial specifications of the DMFC design.

5.1 Initial Exploration and Down-selection

Based upon literature analysis, several basic conceptual morphologies were considered to facilitate a DMFC. In order to provide a pool of basic architectural alternatives for implementation at aircraft level, these concepts were grouped in several general categories: aircraft architectures; propulsion arrangement; drive train concepts; and, core/fan arrangement.

5.1.1 Aircraft Architectures

Four basic aircraft configurations for DMFC application were identified: Conventional Wing-Tube Airframe (CAF); Double-Bubble Fuselage (DBF); Hybrid Wing Body (HWB); and, Strut-braced Wing (SBW). Some particulars include:

- The DBF is a modified CAF with conjunction of two traditional fuselages to create an unconventional lifting body.
- The HWB has a flattened and reflexed airfoil shaped body. A low effective wing loading and beneficial trim effect means a complex high-lift system is not required. The outboard wing supports slats and all trailing edge devices are made up of simple hinged flaps that double as elevons. The distributed propulsion system is mounted atop of the main body, thereby ingesting large portions of the boundary layer (Fig. 13).

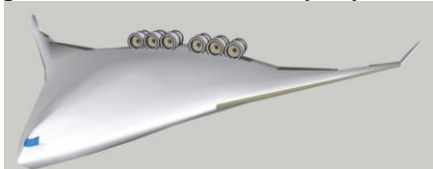


Fig. 13: Hybrid wing body configuration

5.1.2 Drive Train Concepts

Several options of power transmission from the core/turbofan to the fans were investigated.

Transmission concepts were categorised as mechanical, gas-dynamic (gas) and electrical power transmission (Fig. 14).

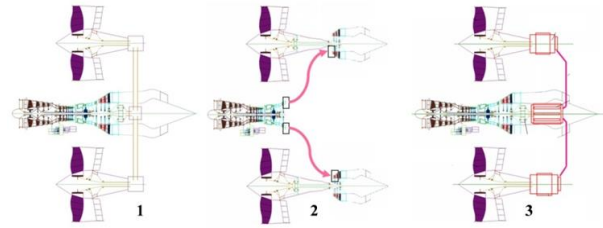


Fig. 14: Power transmission system options (1 – mechanical, 2 – gas, 3 – electrical)

Mechanical Power Transmission

Power extracted from a free turbine shaft located at the core exit provides transmission using shafts and gear boxes to fan rotors. Similar drive-trains exist on modern helicopters, i.e. power extracted from turbo-shaft engine is transmitted to the main and tail rotors.

Gas Power Transmission

Gas extracted from the core exit transfers through gas ducts to individual free turbines connected to fans via shafts. As this type of drive-train has no direct coupling between core and fan shaft it has a substantial amount of transient inertia. This should be taken into account when developing the control system.

Electrical Power Transmission

The electrical generator is mounted on the free turbine shaft at the core exit and generates power using individual electro-motors connected to fans via shafts. Electric power transmission is accomplished using electric wiring. Similar architectures are used for ground-based gas-turbine power stations, where the power is extracted from the gas-turbine to drive electro-generators. Although it appears to be the simplest means of power transmission, even if one takes stock of the high efficiency of electro-motors the large power (some tens of MW) required by the motors makes it a prohibitive solution.

5.1.3 Down-Selection of Candidate Solutions

From the basic architectural alternatives already discussed, 20 initial integrated concepts featuring a multiple fans design were derived. Some other configurations, such as the Box-wing, which were considered in PFC concept pool were not considered here.

Pre-selected concepts are graphically summarised in Fig. 15.

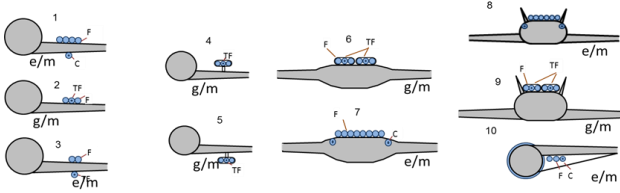


Fig. 15: Distributed multiple fans concept cloud (g – gas-driven, m – mechanically-driven, e – electrically-driven)

Key for Fig. 15

- 1e/m – CAF + fans upper-wing and cores under-wing
- 2g/m – CAF + fans and turbofans upper-wing
- 3e/m – CAF + fans upper-wing and turbofans under-wing
- 4g/m – CAF + pylon-mounted fans and turbofans upper-wing
- 5g/m – CAF + pylon-mounted fans and turbofans under-wing
- 6g/m – HWB + fans and turbofans upper-body
- 7e/m – HWB + fans upper-body and cores embedded within body
- 8e/m – DBF + fans upper-fuselage and cores embedded within fuselage
- 9e/m – DBF + fans and turbofans upper-fuselage
- 10e/m – SBW with distributed multiple fans

From the compilation given above, 8 (CAF and SBW types) out of the initial 20 candidates were discarded due to reasons related to diminished BLI potential. Another goal of the pre-selection was to reduce the pool of candidates down to a manageable number for purposes of closer individual evaluation.

The remaining 12 pre-selected DMFCs were qualitatively rated against the 6 main categories and 29 criteria as discussed in Section 2.1. In Table 3 12 concepts are sorted in order of their scored ranking. Concept 1 had the highest overall rating, thus being the most promising concept for a distributed multiple fans application. In order to evaluate robustness of the concepts, the same procedure as detailed in Section 2.1 was applied.

Table 3: Results of maturity assessment

	Likelihood of success (Drawbacks and Risks)	Effort Req.	Total
5m	4	4	16
5g	4	3	12
6m, 9m	3	3	9
6g, 7m, 8m, 9g, 10e	2	3	6
7e, 8e, 10m	2	2	4

With reference to Table 3 above, Concepts 5m and 5g with CAF were assessed as those with the highest maturity level out of the others. Taking into account the rating of concepts together with maturity assessment results in Table 3 Concept 6m was selected as the best for EIS 2035, and, Concept 7e was selected as best for EIS 2035+.

A graphical summary of rating results is visualised in Fig. 16. In order to allow convenient comparison of the rated concepts, in the presentation of rating results shown in the diagram, the score of the best ranking concept was normalized to 0.50. For purposes of clarity the remaining concepts were scaled accordingly. The bars labeled “Intuition” show the initial results from the concept rating procedure. Additionally, the average value of each robustness scenario is presented.

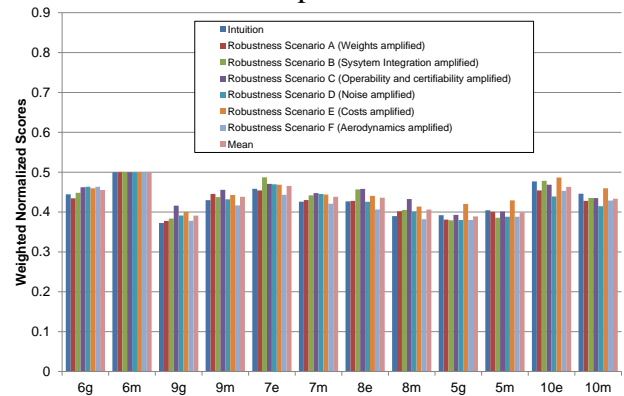


Fig. 16: Results of robustness analysis. Normalised scores for different scenarios

5.2 Aero-Airframe Numerical Experimentation

The investigated configuration is a 2D wing airfoil with a nacelle airfoil, corresponding to a cut of the 3D BWB configuration at a spanwise position corresponding to the engine axis (see Fig. 2 in Section 2.2). The aircraft cruise conditions correspond to M0.80, an altitude FL350, and ISA conditions. It should be noticed that the 2D computations are done at a reduced M0.67 in order to take into account the sweep angle effect of the BWB wing. In this paper, sensitivity studies for different driving geometries or aerodynamic parameters,

performed on this shape and on a preliminary generic shape are only presented.

Fig. 17 shows the effect of a variation in incidence angle, leading to a variation in boundary layer thickness: the total pressure contours illustrate the relative importance of this thickness (local total pressure / freestream total pressure < 0.99 approximately) compared to the engine diameter (D), and also a pressure loss due to a shock wave on the upper side of the wing. All these phenomena contribute to the thrust/drag balance which is quite difficult to establish in these conditions especially for a closely-coupled engine/airframe configuration.

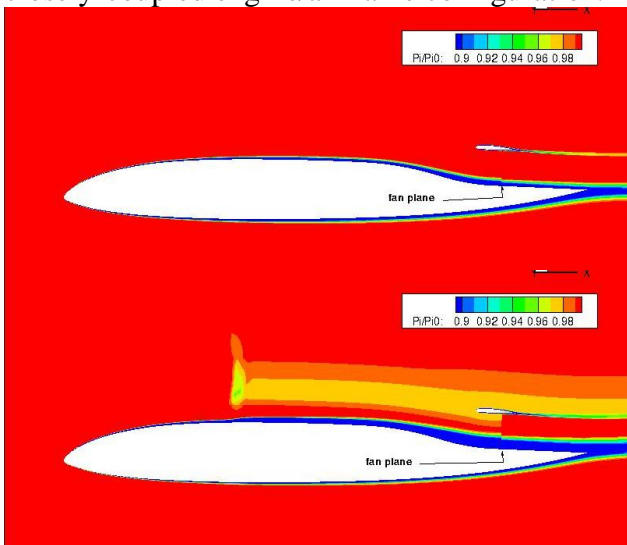


Fig. 17: Evolution of total pressure for incidence 0° (top) and 5° (bottom) at $M0.67$

As illustrated in Fig. 18, a variation in engine thrust or FPR can have a significant effect on the M distributions around the configuration, and as a consequence, on the lift. Another consequence of an FPR increase are higher velocities upstream and inside the engine intake, leading to a reduction in the boundary layer thickness ingested by the intake.

The engine fan diameter, D , is also an important driving parameter, as shown in Fig. 19, for a comparably balanced thrust/drag aerodynamic condition. An increase in D , for a similar value of thrust, corresponds to lower velocities within the intake because the engine mass-flow is higher. As a consequence, the velocities or M on the upper side of the airframe are lower, leading to a reduction in the lift.

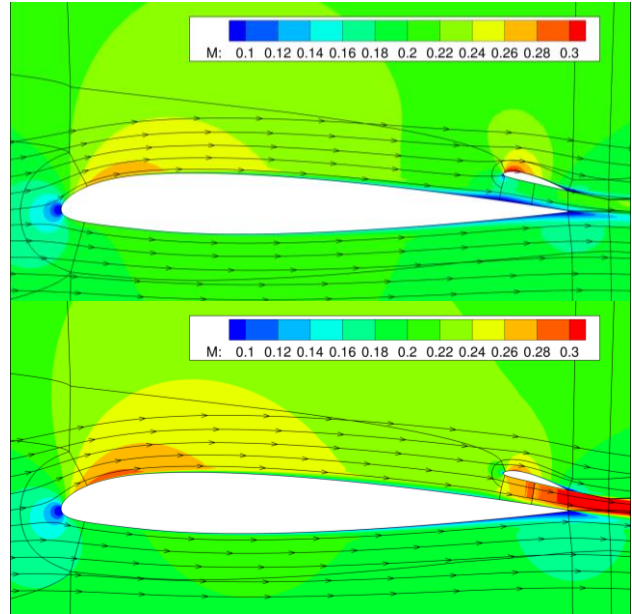


Fig. 18: Mach number distributions for low (top) and high (bottom) Fan Pressure Ratio – generic configuration

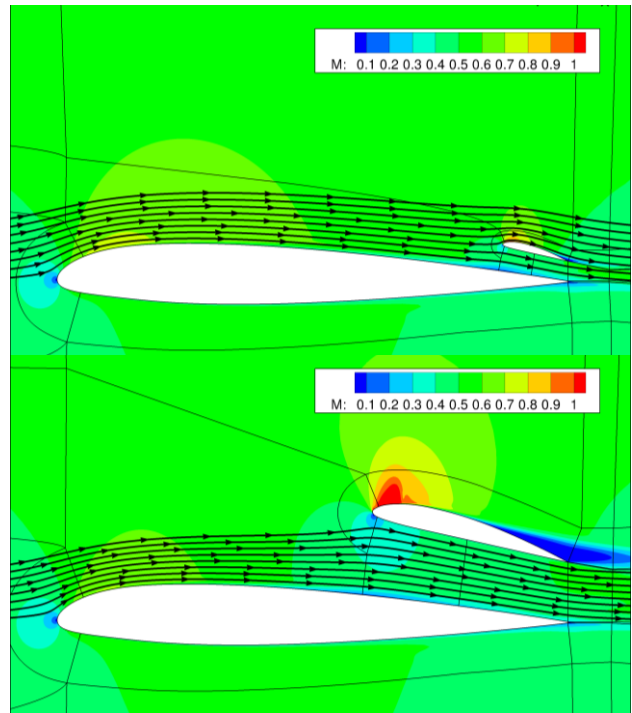


Fig. 19: Mach number distributions for small ($D/c= 0.04$) and large ($D/c= 0.13$) engine for thrust/drag balanced condition – generic configuration; c = wing chord at wing station

The previous conclusions will have to be quantified, in particular in terms of lift and propulsive balance, during the remaining period of the project.

5.3 Initial General Arrangement and Specifications

An initial general arrangement of the baseline HWB is presented in Fig. 20.

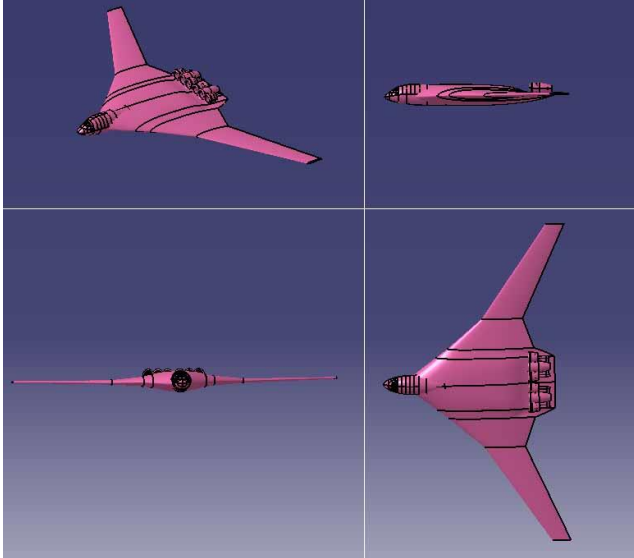


Fig. 20: Initial general arrangement and isometric view of baseline DMFC design

A synopsis of important aircraft characteristics for the selected DMFC design and the 2035R aircraft is given in Table 4.

Table 4: Preliminary comparative synopsis of important aircraft characteristics

		2035R	DMFC*	Δ [%]
Overall Length	m	67.0	37.0	-44.8
Wing Span	m	65.0	65.0	0
MTOW	kg	206230	206500	0.1
OWE	kg	123462	125820	1.9
Wing Ref. Area S_{ref}	m ²	335.4	614.0	83.1
MTOW/ S_{ref}	kg/m ²	615	336	-45.3
Lift-to-Drag Ratio M0.80	-	22.5 ($C_L=0.55$)	24.0 ($C_L=0.30$)	6.7

*if BLI / wake-filling effects are not accounted

6 Conclusion

Details about the latest results of a currently active European Commission funded Framework 7 project entitled Distributed Propulsion and Ultra-high By-Pass Rotor Study at Aircraft Level, or, DisPURSAL have been presented. The technical work covers design and integration considerations related to one unique solution that integrates the fuselage with a single propulsor (dubbed Propulsive-Fuselage Concept, PFC) as well as a Distributed

Multiple-Fans Concept (DMFC) driven by a limited number of engine cores – both targeting entry-in-service year 2035+. The numerical analysis methods for aerodynamic-airframe interaction include high-end, low-fidelity and interlaced-fidelity methods. Work undertaken for both the PFC and DMFC have provided salient insights when it concerns best practise for nacelle overall sizing, nacelle aerofoil section customization and localized aircraft body contouring. The avoidance of localized super-velocities has been identified as one of the principal considerations, especially when inspecting off-design operating conditions. Although this paper reflects work-in-progress developments, initial indications show for a PFC undertaking medium-to-long-range operations an 8.9% reduction in fuel burn and CO₂-emissions compared to an evolutionary, year 2035, conventional morphology gas-turbine aircraft appears to be a worthwhile target.

7 Acknowledgments

Gratitude is conveyed to the following individuals for their contributions to the analysis and work presented in this paper:

- Olivier Altinault, ONERA
- Gerald Carrier, ONERA
- Richard Grenon, ONERA
- Sascha Kaiser, Bauhaus Luftfahrt
- Mario Kalanja, Airbus Group Innovations
- Ulrich Kling, Bauhaus Luftfahrt
- Kay Plötner, Bauhaus Luftfahrt
- Clément Pernet, Bauhaus Luftfahrt
- Alexander Prendinger, undergraduate Masters thesis student Bauhaus Luftfahrt
- Michael Schmidt, Bauhaus Luftfahrt
- Patrick Vratny, Bauhaus Luftfahrt

The research leading to results presented in this paper has received funding from the European Commission Seventh Framework Programme (FP7) through the DisPURSAL Project under Grant Agreement No. 323013.

References

- [1] European Commission, Flightpath 2050 Europe's Vision for Aviation - Report of the High Level Group on Aviation Research, Luxembourg, 2011
- [2] Muller, R. (ASD AeroSpace and Defence Industries Association of Europe), ACARE Goals (AGAPE) Progress Evaluation, Project Final Report Publishable Summary, Support Action Funding Scheme, Proposal No. 205768, European Commission Directorate General for Research and Innovation, June 2010
- [3] Advisory Council for Aviation Research and Innovation in Europe (ACARE), Strategic Research and Innovation Agenda (SRIA) - Volume 1, Brussels, 2012
- [4] Isikveren, A.T., Schmidt, M., "Future Transport Aircraft Ultra-Low Emissions Technology Options", GARS Workshop Air Transport and Climate Change, Worms, Germany, 4 April 2014
- [5] Isikveren, A.T. (Bauhaus Luftfahrt e.V.), "Distributed Propulsion and Ultra-high By-pass Rotor Study at Aircraft Level (DisPURSAL)", FP7-AAT-2012-RTD-L0, Proposal No. 323013, European Commission Directorate General for Research and Innovation, 14 March 2012
- [6] Mistree, F., Lewis, K., Stonis, L., "Selection in the Conceptual Design of Aircraft", AIAA-94-4382-CP, 32nd AIAA Aerospace Sciences Meeting and Exhibit, Reno, NV, January 10-13, 1994
- [7] Steiner, H.-J., Seitz, A., Wiczorek, K., Plötner, K., Isikveren, A.T., Hornung, M., "Multi-Disciplinary Design and Feasibility Study of Distributed Propulsion Systems," in 28th International Congress of the Aeronautical Sciences (ICAS), 2012.
- [8] Cambier, L., Heib, S., Plot, S., "The Onera elsA CFD software: input from research and feedback from industry", *Mechanics and Industry Journal*, Vol. 14, Issue 03, pp. 159-174, April 2013
- [9] Atinault, O., Carrier, G., Grenon, R., Verbecke, C., Viscat, P., "Numerical and Experimental Aerodynamic Investigations of Boundary Layer Ingestion for Improving Propulsion Efficiency of Future Air Transport", AIAA 2013-2406, 31st AIAA Applied Aerodynamics Conference, San Diego, CA, 2013
- [10] Seitz, A., Gologan, C., "Parametric Design Studies for Propulsive Fuselage Aircraft Concepts", Paper No. 257, 4th CEAS Air and Space Conference, 2013, Linköping, Sweden, September 2013
- [11] Seitz, A., Bijewitz, J., Kaiser, S., Wortmann, G., "Conceptual Investigation of a Propulsive Fuselage Aircraft Layout", *Aircraft Engineering and Aerospace Technology: An International Journal*, Vol. 6, Number 86, to be published in October 2014
- [12] AERO2k, Global Aviation Emissions Inventories for 2002 and 2025, website: http://aero-net.info/fileadmin/aeronet_files/links/documents/AERO2K_Global_Aviation_Emissions_Inventories_for_2002_and_2025.pdf, cited June 2013
- [13] Official Airline Guide (OAG), Historical Data, 2012
- [14] Bolonkin, A., "A high efficiency fuselage propeller ('Fuselan') for subsonic aircraft," in World Aviation Conference, San Francisco, 1999
- [15] Stückl, S., van Toor, J., Lobentanzer, H., "VoltAir – The All Electric Propulsion Concept Platform – A Vision for Atmospheric Friendly Flight," in 28th International Congress of the Aeronautical Sciences (ICAS), 2012
- [16] Schwarze, M., Zold, T., "Angepasste Flugzeugkonfigurationen für die Energieeffiziente Open-Rotor Integration auf zukünftigen Kurzstrecken-Verkehrsflugzeugen", Document ID. 301447, Deutscher Luft- und Raumfahrtkongress 2013, Stuttgart, September 2013
- [17] Isikveren, A.T., Seitz, A., Vratny, P.C., Pomet, C., Plötner, K., Hornung, M., "Conceptual Studies of Universally-Electric Systems Architectures Suitable for Transport Aircraft", Paper No. 1368, Deutscher Luft- und Raumfahrtkongress 2012, Berlin, September 2012
- [18] Raymer, D., et al., "Advanced Technology Subsonic Transport Study. N+3 Technologies and Design Concepts", NASA TM-2011-217130, 2011

8 Contact Author Email Address

Askin T. Isikveren
Head of Visionary Aircraft Concepts
Bauhaus Luftfahrt e.V.
Lyonel-Feininger-Str. 28
80807 Munich, Germany
Email: askin.isikveren@bauhaus-luftfahrt.net

Copyright Statement

The authors confirm that they, and/or their company or organization, hold copyright on all of the original material included in this paper. The authors also confirm that they have obtained permission, from the copyright holder of any third party material included in this paper, to publish it as part of their paper. The authors confirm that they give permission, or have obtained permission from the copyright holder of this paper, for the publication and distribution of this paper as part of the ICAS 2014 proceedings or as individual off-prints from the proceedings.